

# Nondestructive Characterization and In-situ Monitoring of Corrosion Degradation by Backward Radiated Ultrasound

†Sung-Jin Song<sup>1</sup>, Young H. Kim<sup>1</sup>, Dong-Ho Bae<sup>1</sup>, and Sung D. Kwon<sup>2</sup>

<sup>1</sup>*School of Mechanical Engineering, Sungkyunkwan University, Suwon, KOREA*

<sup>2</sup>*Department of Physics, Andong National University, Andong, KOREA*

Since the degradation caused by corrosion is restricted to the surface of materials, conventional ultrasonic nondestructive evaluation methods based on ultrasonic bulk waves are not applicable to characterization of the corrosion degradation. To take care of this difficulty, a new nondestructive evaluation method that uses ultrasonic backward radiation has been proposed recently. This paper explores the potential of this newly developed method for nondestructive characterization and in-situ monitoring of corrosion degradation. Specifically, backward radiated ultrasounds from aged thermo-mechanically controlled process (TMCP) steel specimens by corrosion fatigue were measured and their characteristics were correlated to those of the aged specimens. The excellent correlation observed in the present study demonstrates the high potential of the backward radiated ultrasound as an effective tool for nondestructive characterization of corrosion degradation. In addition, the potential of the backward radiated ultrasound to in-situ monitoring of corrosion degradation is under current investigation.

**Keywords** : *ultrasound, backward radiation, corrosion degradation, nondestructive characterization, in-situ monitoring*

## 1. Introduction

Corrosion is one of the major failure mechanisms that cause degradation of various engineering materials and structures so that in-situ monitoring and nondestructive characterization of corrosion degradation become very important tasks in structural integrity evaluation. Since the degradation caused by corrosion (or corrosion fatigue) is heavily restricted to the surface of materials conventional ultrasonic nondestructive evaluation (NDE) methods based on ultrasonic bulk waves (such as longitudinal wave and shear wave) are not suitable to the quantitative characterization of corrosion degradation. To take care of this difficulty, a new NDE method that uses ultrasonic backward radiation has been proposed recently.<sup>1,2)</sup>

Rayleigh surface waves that can propagate to some depth below the surface (approximately, one wavelength) with exponential profiles are very suitable to interrogate such corrosion degradations that are localized to the surface with subsurface gradients. When a broadband pulse (generated from a transmitting transducer) is incident at an arbitrary oblique angle to the surface of test piece (immersed in water), Rayleigh surface wave propagates

along the surface if the phase of the incident beam matches that of Rayleigh surface wave. If there are some scatterers (such as grain boundaries, micro cracks and pits, and the end of test piece), the Rayleigh wave will be scattered (or reflected) backwardly to propagate to the opposite direction. A portion of energy of scattered Rayleigh wave leaks to water, and it reaches to the transmitting transducer. The wave returning back to the transmitting transducer is usually called as the "backward radiated ultrasound" or the "backscattered ultrasound."

The backward radiated ultrasound contains the information related to the perturbations in the surface where the Rayleigh wave propagates. Previous studies showed that the backward radiated ultrasound can be used to assess the perturbations in microstructures,<sup>1)</sup> and in wear-in procedure.<sup>2)</sup>

In the present work, the characteristics of Rayleigh surface wave propagating in the aged specimens due to corrosion fatigue are investigated by measuring the profiles of backward radiated ultrasound. The Rayleigh surface wave velocities and their dispersion were obtained from the backward radiation profiles, and they were correlated to the corrosion-fatigue characteristics of the interrogated specimens for the quantitative, nondestructive characterization of corrosion degradation. In addition, the

†Corresponding author: sjsong@yurim.skku.ac.kr

potential of the backward radiated ultrasound to in-situ monitoring of corrosion degradation is investigated by the experiments in laboratory.

## 2. Theoretical background

The backward radiated ultrasound is leaky ultrasonic wave returning back to a transmitting transducer (along the opposite direction to the incident beam) from the backward propagating leaky surface wave, which is converted from the forward surface wave generated in the incident surface region. Let us consider the ultrasound that is incident on a specimen immersed in water. When ultrasound is incident at a certain angle (near the Rayleigh critical angle), Rayleigh surface wave is generated by mode conversion and propagates along the plate and reflected at the specimen edge. A portion of its energy leaks into water to be detected by the transmitting transducer. In pulse-echo measurements of ultrasonic backward radiation, there can be captured three responses including: 1) direct scattering at the incident position, 2) leak of the Rayleigh surface wave propagating backward due to microstructures and 3) leak of the Rayleigh surface wave reflected at the specimen edge. Among them, the last one (which is often called the "averaging method") provides the highest amplitude to be detected and processed without spatial averaging. In the present work, therefore, we adopt the averaging method in order to evaluate the degradation of specimens.

Previously, Kwon *et al.*<sup>3)</sup> have discussed various factors (including beam directivity, the frequency characteristics of the transducer, dispersion and scattering of surface waves) that can alter the characteristics of backward radiation, and proposed an equation that can describe the angular profile of backward radiation amplitude,  $V(\theta)$ , as given by Eq. (1).

$$V(\theta) = A \int_0^{\infty} T(f) C(f, d) [D(\theta - \theta_f)]^2 df \quad (1)$$

where  $f$  is frequency,  $A$  is a proportional constant,  $T(f)$  represents the frequency characteristics of transducer,  $\theta$  denotes the incidence angle of beam center,  $D(\theta)$  represents the directivity of transducer,  $C(f, d)$  is the conversion function from forward to backward wave,  $d$  is the scatter size, and  $\theta_f$  is the angular dispersion function. More detailed explanation for these parameters can be found in Kwon *et al.*<sup>3)</sup> which has pointed out that the width of the profile is related to the severity of dispersion of the substrate and the peak intensity is inversely proportional to the width of the profile.

## 3. Experiments

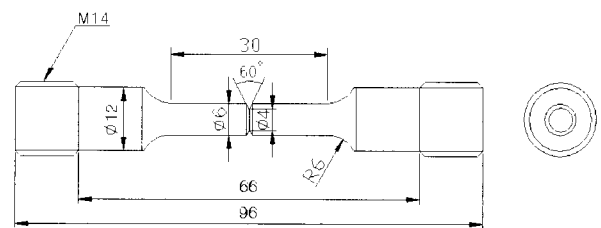
### 3.1 Specimens and Procedure

Table 1 illustrates the chemical compositions and mechanical properties of thermo-mechanically controlled process (TMCP) steel used in this study. Fig. 1 shows the dimensions of the specimens fabricated in the present study. An artificial notch was machined on the specimen, and a corrosion fatigue test was carried out in synthetic seawater (25 °C, 3.5 wt.% NaCl solution). Since the asperity and oily particles on the surface of the specimen affect corrosion reaction of metals, the surface of specimens was polished and then cleaned with an ultrasound washer.

A horizontal type of a hydraulic corrosion fatigue tester (the maximum capacity of 20 kN) was fabricated in order to relax the problems caused by vertical type testers. The corrosion cell as shown in Fig. 2 was fabricated with acryl for providing constant corrosive environment (temperature, pressure and etc.) without galvanic corrosion during the test period. The synthetic seawater was circulated by the rate of 50 ml/min. A sinusoidal load of 1.0 Hz was applied to the specimens. The minimum load ( $P_{min}$ ) has been kept to be equal to 10% of the maximum load ( $P_{max}$ ). Table 2 summarizes the loading conditions, ( $P_{max}$ ,  $P_{min}$  and  $\Delta P = P_{max} - P_{min}$ ), the number of cycles to failure,  $N_f$ , and the period exposed to the corrosion environment,  $T_{cor}$ , that have been applied to six different specimens (identified by from "A" to "F").

**Table 1. Chemical composition and mechanical properties of TMCP steel**

| Element              | C                    | Mn   | Si             | P     | S     | Cu    | Ni   |
|----------------------|----------------------|------|----------------|-------|-------|-------|------|
| Content (%)          | 0.10                 | 1.49 | 0.25           | 0.014 | 0.001 | 0.024 | 0.25 |
| Yield strength (MPa) | Youngs Modulus (GPa) |      | Elongation (%) |       |       |       |      |
| 519                  | 228                  |      | 34.2           |       |       |       |      |



**Fig. 1. Schematic diagram of the specimen.**

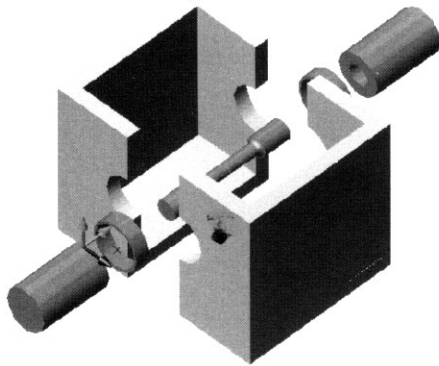


Fig. 2. Corrosion cell for Corrosion fatigue test

Table 2. The loading condition and number of cycles to failure for the specimens.

| Specimen ID | $P_{max}$ (MPa) | $P_{min}$ (MPa) | $\Delta P$ (MPa) | $N_f$   | $T_{cor}$ (hour) |
|-------------|-----------------|-----------------|------------------|---------|------------------|
| A           | 222.2           | 22.2            | 200.0            | 37,438  | 10.4             |
| B           | 197.1           | 19.7            | 177.4            | 62,482  | 17.4             |
| C           | 172.2           | 17.2            | 155.0            | 122,553 | 34.0             |
| D           | 147.8           | 14.8            | 133.0            | 252,350 | 70.1             |
| E           | 123.3           | 12.3            | 111.0            | 262,900 | 73.0             |
| F           | 98.6            | 9.9             | 88.7             | 598,432 | 166.2            |

### 3.2 Ultrasonic measurement system

The experimental setup adopted in the present study for the automated measurement of ultrasonic backward radiation is shown in Fig. 3. The specimen holder can be translated and rotated in order to control the point and angle of incidence for scanning over the specimen. Three micro-step motors were employed for these movements and controlled by a personal computer. The accuracies in rotating angle and translation displacement were  $0.01^\circ$  degree and 0.05 mm, respectively. A broadband ultrasonic transducer (with the center frequency of 5 MHz) was used to interrogate the specimen at different angles of incidence. A computer controlled ultrasonic pulser/receiver was used to generate the Rayleigh surface waves at and near the Rayleigh angle of incidence. A portion of the surface wave scattered backwardly, whereas the remained portion propagated forwardly and reflected at the edge of the specimen to propagate backwardly. A certain portion of backward propagating energy leaks back along the incident direction toward the transmitting transducer. The received backscattering signals captured by the transducer were then digitized by a digital oscilloscope and transferred to

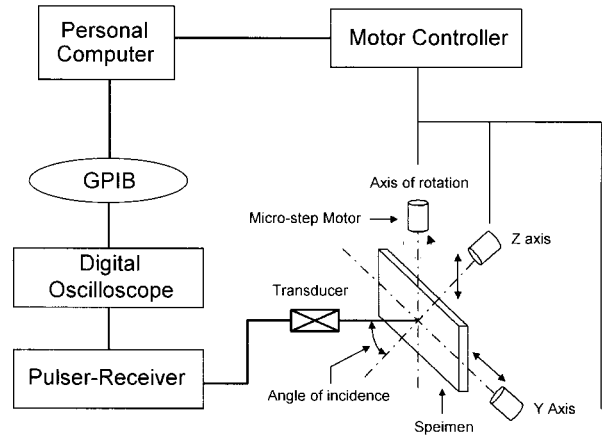


Fig. 3. Schematic diagram of the experimental setup.

a personal computer. The rf waveforms and frequency spectra of backward radiation ultrasound were stored and analyzed. In order to make the reflection condition from the edges consistent throughout the specimens, the ends of all specimens were cut vertically by electric discharge machining.

### 4. Nondestructive characterization of corrosion degradation

The typical rf waveforms obtained at the incident angles of  $27.6^\circ$ ,  $28.0^\circ$ ,  $28.4^\circ$  and  $29.2^\circ$  for the specimen "C" are shown in Figs. 4(a), (b), (c) and (d), respectively. The rf signals contains 4 different responses which are identified by from (1) to (4) as shown in Fig. 4(c). The corresponding beam paths for the four responses are shown in Fig. 5 schematically. The response marked by (1) in Fig. 4(c) is corresponding to the direct backscattering near the incident region as shown in Fig. 5(a), and the response marked by (2) are the leaks of Rayleigh surface wave due to the presence of microscopic scatterers as shown in Fig. 5(b).

The response marked by (3) is the leak of Rayleigh surface wave propagating backwardly due to the reflection at the edge of specimen as shown in Fig. 5(c). Finally, the response marked by (4) is the leaks of the Rayleigh surface waves due to the multiple reflection and scattering as shown in Fig. 5(d). The amplitude of the backscattering ultrasound marked by (3) in Fig. 4(c),  $V(\theta)$ , is a function of the incident angle, and it showed the maximum at the incident angle of  $28.4^\circ$ .

In the present work, the backscattering waveforms from the six specimens were captured successively with varying the incident angle continuously to measure the amplitude of the backscattering ultrasound,  $V(\theta)$ , experimentally. Fig.

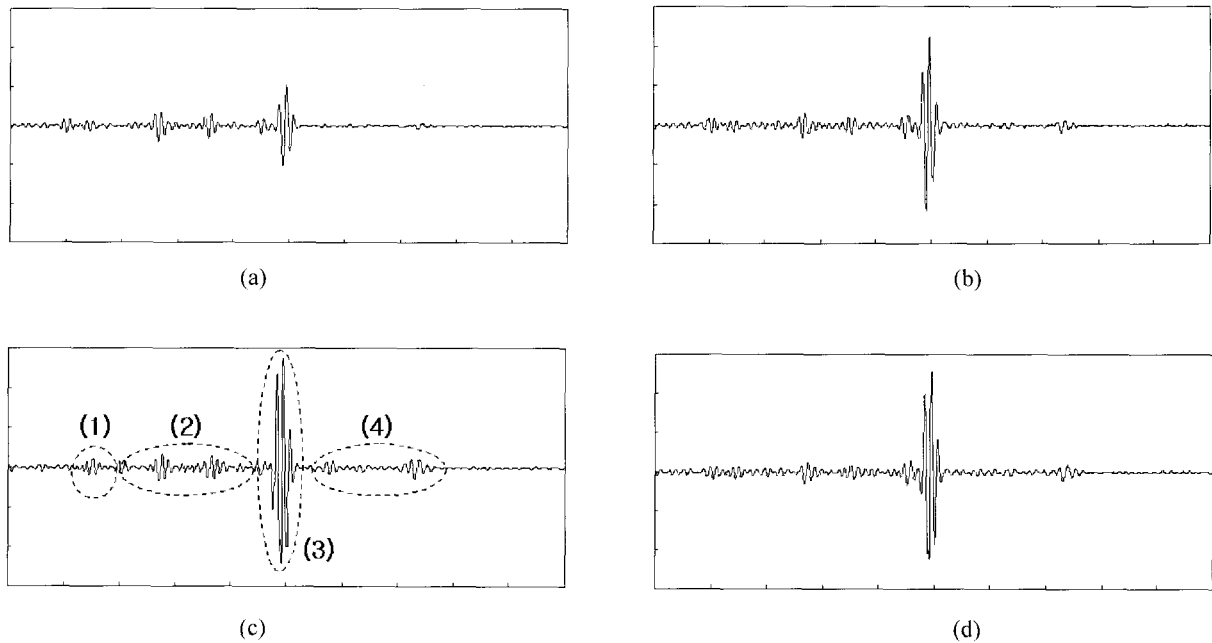


**Fig. 4.** Typical rf waveforms obtained at the incident angles of (a)27.6°, (b)28.0°, (c)28.4° and (d)29.2° for the specimen C. (Hor: 2μ s/div, ver: 1V/div).

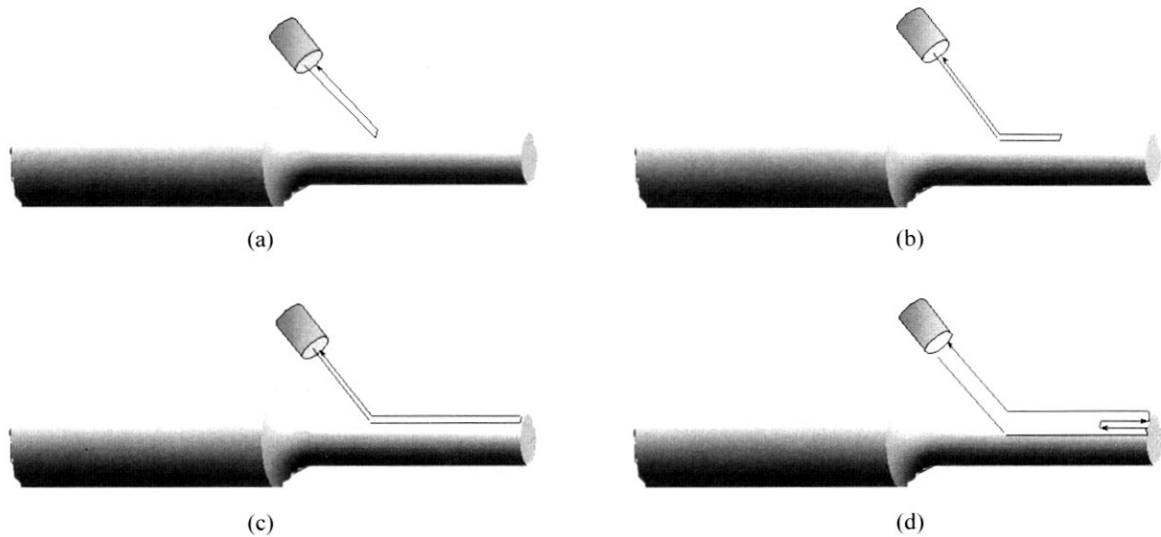


**Fig. 5.** Possible beam paths near the Rayleigh critical angles. (a) direct backscattering near the incident region, (b) leak of the Rayleigh surface wave due to the scattering from the microstructures, (c) leak of the Rayleigh surface waves due to the reflection at the edge of the specimen and (d) leak of the Rayleigh surface waves due to the multiple reflection and scattering.

6 shows the result of this measurement carried out to the six specimens. In the measurement, it was observed that the absolute magnitude of the signal was very sensitive to various factors (including the alignment of the cylindrical specimen, and the distance from the incident position to the specimen edge) so that it is really difficult to have discussion based on the absolute value of the

profile. Therefore, each profile was normalized by the maximum value of the profile so that all the profiles have almost the same height (Fig. 6). The Rayleigh surface wave was most efficiently generated at the incident angle which was corresponding to the maximum value of the backscattering profile,  $\theta_p$ . Thus, the velocity of Rayleigh surface wave,  $c_R$ , can be determined using the value of

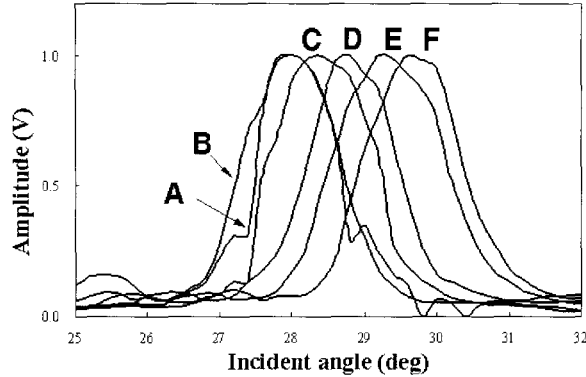


Fig. 6. Backscattering profiles of the Rayleigh surface wave for the corrosion-fatigue specimens.

Table 3. The incident angle for peak profile, width of the profile and corresponding surface wave velocities.

| Specimen ID | $T_{cor}$ (hour) | $\theta_p$ (Degree) | $\theta_w$ (degree) | $c_R$ (m/s) |
|-------------|------------------|---------------------|---------------------|-------------|
| A           | 10.4             | 28.0                | 1.27                | 3,150       |
| B           | 17.4             | 28.0                | 1.48                | 3,150       |
| C           | 34.0             | 28.4                | 1.69                | 3,110       |
| D           | 70.1             | 28.8                | 1.42                | 3,070       |
| E           | 73.0             | 29.2                | 1.80                | 3,030       |
| F           | 166.2            | 29.6                | 1.59                | 3,000       |

$\theta_p$ . In addition, we have defined the width of the profile,  $\theta_w$ , as the distance between two points on the profile where the amplitude dropped to a half of its peak, in order to investigate the dispersion characteristics of Rayleigh surface wave.

The values of  $\theta_p$ ,  $\theta_w$  and  $c_R$  for the six specimens are listed in Table 3, and the relationships among them are presented graphically in Figs. 7 and 8. The relation between  $c_R$  and  $N_f$  is given in Fig. 7, while that between  $\theta_w$  and  $N_f$  is in Fig. 8. As the increase of  $N_f$ ,  $c_R$  becomes slower while  $\theta_w$  become larger. The behaviors can be explained by recalling the case of having an effective degraded layer with less acoustic impedance.<sup>4)</sup> The typical subsurface gradients caused by corrosion aging are in a form of exponential functions with respect to the depth. For the simplification of our discussion, however, one can assume that a single, effective degraded layer has been developed in the surface of a specimen. Under such a simplification, the dispersion curve and its slope decrease as the increase of the product of frequency multiplied by thickness of the effective layer.<sup>5)</sup> Therefore, as the increase

of the degraded layer thickness, the Rayleigh wave velocity (which is corresponding to the peak angle of a backscattering profile) decreases whereas the profile width increases. It is well known that the severer corrosion environment yields the thicker layer, which corresponds to the larger  $\theta_p$  and the less  $c_R$ .<sup>4)</sup> In fact, the expected behavior, i.e. the increase of  $\theta_w$  according to the increase of the number of cycles to failure,  $N_f$ , can be observed in Fig. 8. The degraded layer for the specimen F (with severer degradation) is expected to be thicker than that of the specimen A (with less degradation). It is reasonable to assume that the amount of corrosion is proportional to the product of the corrosion time multiplied by corrosion rate, and the corrosion rate would be accelerated by the applied stress. Therefore, the load applied to the specimen would increase the corrosion rate in the notched region (where the stress concentration occurred) and, as a result, it would decrease the number of cycles to failure,  $N_f$ , by increasing the corrosion rate in addition to the mechanical fatigue. However, in the other region of the

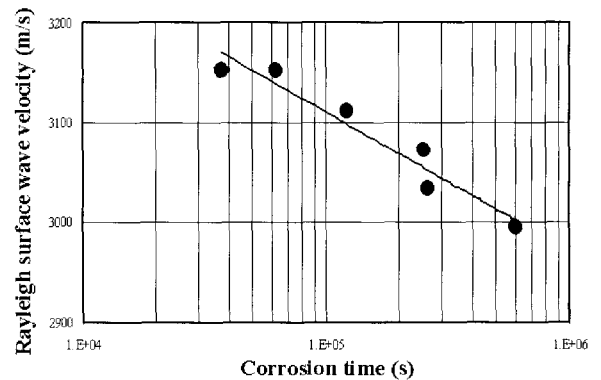


Fig. 7. Relationship between Rayleigh surface wave velocity and period under the corrosion.

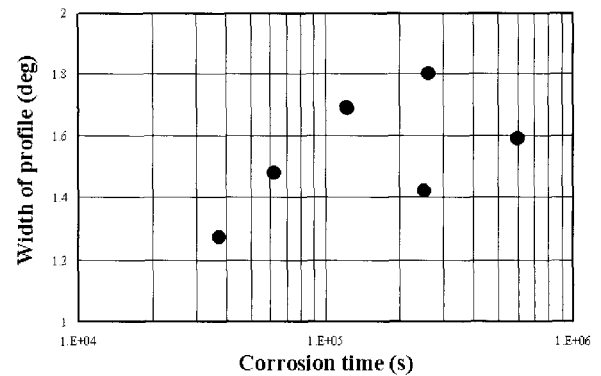


Fig. 8. Relationship between the profile width and the period under the corrosion.

specimen (where the ultrasonic measurement performed), the increase of the corrosion rate due to the increase of the applied stress seemed to be not so profound that the amount of corrosion decreased even with the increase of the applied load. In fact, the amount of corrosion increased according to the increase of the corrosion time,  $T_{cor}$ . This implies that the amount of corrosion is dominantly determined by the corrosion time in this specific corrosion fatigue test.

### 5. In-situ monitoring of corrosion degradation

For the nondestructive characterization of corrosion degradation discussed in the above section, a series of corrosion fatigue tests have been made separately a prior to the ultrasonic backward radiation measurements. Unfortunately, however, this two-step approach cannot be applied to the evaluation of most materials or structures that are under service. For such materials or structures under service, in-situ monitoring of corrosion degradation is much more suitable. In the in-situ monitoring, backward radiated ultrasound has to be measured directly from test pieces under corrosion environments. To explore the potential of backward radiated ultrasound to in-situ monitoring, a series of experiments are currently carried out using a chamber (as shown in Fig. 9 schematically)

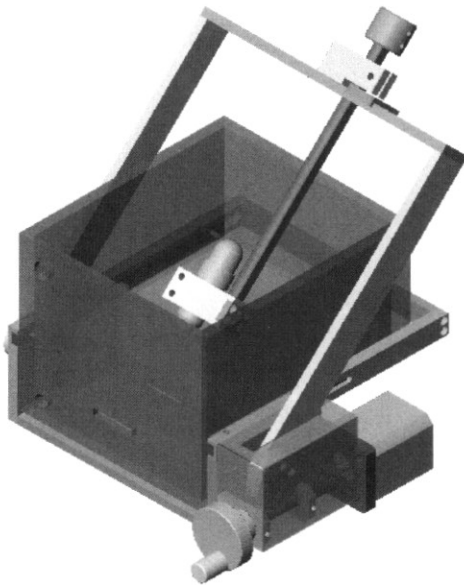


Fig. 9. Schematic representation of a chamber fabricated for in-situ monitoring of degradation caused by corrosion fatigue

that has been fabricated for in-situ monitoring of degradation caused by corrosion fatigue. This chamber can hold a specimen (that is under loading by a horizontal fatigue tester) immersed in corrosive solution and the ultrasonic transducer to capture the backward radiated ultrasonic signals. The results of this experimental investigation will be reported shortly.

### 6. Conclusion

In the present study, the corrosion degradation characteristics of the TMCP steel have been investigated nondestructively by analyzing the backward radiation profiles of Rayleigh surface waves that were measured from the six corrosion-fatigue specimens with various loading magnitude. The velocity of Rayleigh surface wave decreased and the width of the profile increased with the increase of the time exposed to the corrosion environment. The measurement results implied that the effective thickness of the degraded layer with less acoustic impedance increased according to the increase of corrosion time. The results observed in this study demonstrate high potential of the backward radiated ultrasound to serve as an effective tool for nondestructive evaluation of the subsurface degradation characteristics due to corrosion fatigue. In addition, to explore the potential of backward radiated ultrasound to in-situ monitoring, a series of experiments are currently carried out using a chamber that has been fabricated for in-situ monitoring of degradation caused by corrosion fatigue. The results of this experimental investigation will be reported shortly.

### References

1. H. C. Kim, J. K. Lee, S. Y. Kim, and S. D. Kwon, *Japanese Journal of Applied Physics*, **38**, 260 (1999).
2. S. D. Kwon, S. J. Song, D. H. Bae, and Y. Z. Lee, *KSME International Journal*, **16**, 1084 (2002).
3. S. D. Kwon, M. S. Choi, and S. H. Lee, *NDT&E International*, **33**, 275 (2000).
4. T. L. Szabo, *Journal of Applied Physics*, **46**, 1448 (1975).
5. S. D. Kwon, S. S. Yoon, S. J. Song, and D. H. Bae, Review of Progress in Quantitative Nondestructive Evaluation, Vol.20, D. O. Thompson and D. E. Chimenti (Eds.), p.1437, AIP, New York, 2001.